The Astrophysical Journal, 870:21 (8pp), 2019 January 1 https://doi.org/10.3847/1538-4357/aaee7d

Laboratory Measurements of X-Ray Emission from Highly Charged Argon Ions

Esra Bulbul[1,2], Adam Foster[2], Gregory V. Brown[3], Mark W. Bautz[1], Peter Beiersdorfer[3], Natalie Hell[3], Caroline Kilbourne[4], Ralph Kraft[2], Richard Kelley[4], Maurice A. Leutenegger[4,5], Eric D. Miller[1], F. Scott Porter[4], and Randall K. Smith[2]
[1] Massachusetts Institute of Technology, Kavli Institute for Astrophysics & Space Research, 77 Massachusetts Avenue, Cambridge, MA 02139, USA
ebulbul@cfa.harvard.edu
[2] Harvard-Smithsonian Center for Astrophysics, 60 Garden Street, Cambridge, MA 02138, USA
[3] Lawrence Livermore National Laboratory, 7000 East Avenue, Livermore, CA 94550, USA
[4] NASA Goddard Space Flight Center, 8800 Greenbelt Road, Greenbelt, MD 20771, USA
[5] Department of Physics, University of Maryland Baltimore County, 1000 Hilltop Circle, Baltimore, MD 21250, USA
Received 2018 March 9; revised 2018 September 25; accepted 2018 November 2; published 2018 December 28

Abstract

Uncertainties in atomic models will introduce noticeable additional systematics in calculating the flux of weak dielectronic recombination (DR) satellite lines, affecting the detection and flux measurements of other weak spectral lines. One important example is the Ar XVII Heβ DR, which is expected to be present in emission from the hot intracluster medium of galaxy clusters and could impact measurements of the flux of the 3.5 keV line that has been suggested as a secondary emission from a dark matter interaction. We perform a set of experiments using the Lawrence Livermore National Laboratory's electron beam ion trap (EBIT-I) and the X-ray Spectrometer quantum calorimeter (XRS/EBIT) to test the Ar XVII Heβ DR origin of the 3.5 keV line. We measured the X-ray emission following resonant DR onto helium-like and lithium-like Argon using EBIT-I's Maxwellian simulator mode at a simulated electron temperature of $T_e = 1.74$ keV. The measured flux of the Ar XVII Heβ DR lined is too weak to account for the flux in the 3.5 keV line, assuming reasonable plasma parameters. We, therefore, rule out Ar XVII Heβ DR as a significant contributor to the 3.5 keV line. A comprehensive comparison between the atomic theory and the EBIT experiment results is also provided.

Key words: atomic data – line: identification – methods: laboratory: atomic – techniques: spectroscopic – X-rays: galaxies: clusters

1. Introduction

Since its discovery, the nature of dark matter has been one of the prime problems of physics. A range of exotic particles, which could constitute the dark matter content of the universe, have been widely investigated by ground- and space-based direct and indirect searches. Observations of dark matter-dominated objects with space telescopes provide an avenue for indirect detection of secondary emission from dark matter interactions. An intriguing detection of an emission line at ~3.5 keV has been reported by Bulbul et al. (2014a) in the stacked observations of clusters of galaxies and in many other dark matter-dominated objects (Boyarsky et al. 2014, 2015; Urban et al. 2015; Bulbul et al. 2016; Franse et al. 2016; Neronov et al. 2016; Cappelluti et al. 2017). The origin of the emission line is still under discussion, with one proposal being that the X-rays are produced by the secondary emission of dark matter particles (e.g., Conlon et al. 2016; Abazajian 2017). Alternative astrophysical origins of the unidentified line have been extensively discussed in Bu14a and Gu et al. (2015), one of which is the possibility that it results from an unexpectedly strong dielectronic recombination (DR) satellite line created when He-like Ar^{16+} recombines to form Li-like Ar^{15+}. Uncertainties on the atomic calculations of weak satellite lines, such as the Ar XVII Heβ DR transition $1s\ 2p\ 3p\ ^2D_{5/2} \rightarrow 1s^2 2p\ ^2P_{3/2}$, may introduce unknown systematics on the measured flux of the 3.5 keV line and provide an alternative explanation of the origin of the line (Bulbul et al. 2014a, 2014b, hereafter B14b). Measurements performed using the electron beam ion trap (EBIT-I; Levine et al. 1988; Marrs et al. 1988; Beiersdorfer et al. 2003; Beiersdorfer 2008; Marrs 2008), located at Lawrence Livermore National Laboratory (LLNL), provide an avenue for testing the Ar XVII Heβ DR origin of the 3.5 keV line and evaluation of the atomic databases, e.g., AtomDB v2.0.2 and FAC (Foster et al. 2012). Using a unique operating mode, the EBIT-I generates a quasi-Maxwellian distribution of electron energies (Savin et al. 2000, 2008) at electron temperatures similar to those found in astrophysical objects in thermal equilibrium. Measurements using this mode have been used to test atomic theory for highly charged ions of iron (Gu et al. 2012) and gold (May et al. 2004, 2005). In addition, the accuracy of the Maxwellian generator has also been tested using well-known intensity ratios from helium-like ions (Savin et al. 2000, 2008) and hydrogen-like ions (Gu et al. 2012). Measurements using this mode include all relevant population processes in a complete way, i.e., there is no limit to the number of transitions that are included, unlike in computer models. We have used this mode to generate an argon plasma at $kT_e \sim 1.7$ keV and to measure the emission using a high-resolution quantum calorimeter, which is similar to the Soft X-ray Spectrometer (Kelley et al. 2016) flown on the *Hitomi* X-ray Observatory (Takahashi et al. 2016), which includes all line emission from K-shell transitions in highly charged argon spanning the 3–4 keV band. These measurements include emission from the Ar XVII He-α complex Ar XVIII Lyα, and Ar XVII He-β, γ, δ, and ϵ lines, with their relative intensities to the He-like Ar XVII He-α resonance line at 3.12 keV. These new measurements are complementary to measurements conducted earlier using a high-resolution crystal spectrometer attached to the Princeton Large Torus (Beiersdorfer et al. 1995). In that work, the authors measured the $K\beta$ line of He-like Ar^{16+} in the energy range of 3.54–3.71 keV and successfully identified Ar XVI lines produced by DR from Ar^{16+} to Ar^{15+}, as well as lines from electron impact excitation

(the latter not only from He-like Ar^{16+}, but also from lithium-like Ar^{15+} and beryllium-like Ar^{14+}). Here, we use the EBIT-I to measure directly the spectrum of highly charged argon ions in a simulated Maxwellian plasma (see Section 2) that reaches down to 3 keV. Using the data from both the new measurements and from those of Beiersdorfer et al. (1995), a stringent test of the models used by B14a is completed. We compare the line ratios measured by the new EBIT measurements with the observed line ratios in *XMM-Newton* and *Chandra* observations of stacked clusters where the unidentified line has been observed with the highest significance.

This paper is organized as follows. We provide details of the EBIT-I experiment design in Section 2. In Section 3, we provided details of the atomic models used: because the older version of AtomDB v2.0.2 used in B14a cannot analyze the EBIT-I plasma, we include here a comparison between the AtomDB versions. The analysis in Section 4 compares the EBIT-I spectrum with the flexible atomic code (FAC) and AtomDB v3.0.8 models, then explores the effects of these results on the discoveries in B14a. We finally summarize our conclusion in Section 5. All errors quoted throughout the paper correspond to 68% single-parameter confidence intervals.

2. Experiment Design

The results presented here are measured using EBIT-I's Maxwellian simulation mode (Savin et al. 2000, 2008). In this mode, the electron beam is "swept" in a voltage pattern that, when averaged over several cycles, corresponds to a Maxwell–Boltzmann electron distribution at an experimentally controlled temperature. The electron beam energy is "swept" from below the threshold for any relevant process that may contribute to the line emission of interest, such as low-energy DR resonances, up to electron energies $\geqslant$6 times the simulated temperature. For example, for the $\sim$2 keV plasma presented here where the focus is on K-shell emission from highly charged argon ions and where all the relevant dielectronic resonance energies are above 2 keV, the beam is swept from 1.5 keV up to 24 keV. The electron density for this measurement is $\sim 10^{11}$ cm^{-3}. One caveat of the Maxwellian mode is that the plasma generated in the EBIT has a lower average charge than a plasma in true thermal equilibrium, thus intensities of line emission from different ions will not be representative of a Maxwellian plasma. However, the relative intensities of emission lines whose excited states are dominated by processes involving a single ion, such as ratios of two He-like lines or of a resonance line and a DR satellite from the same parent charge state, are the same as found in a true Maxwell–Boltzmann plasma (Savin et al. 2000, 2008; Gu et al. 2012). This is supported by the results presented here for both He-like argon and H-like argon.

The spectra are measured using the X-ray Spectrometer (XRS)/EBIT quantum calorimeter (Porter et al. 2000, 2004), designed and built at the NASA Goddard Space Flight Center. The XRS/EBIT is an energy-dispersive spectrometer with an energy resolution of $\Delta E \sim 5$ eV, a bandwidth that spans the range from below 500 eV to about 10 keV, and a quantum efficiency of 100% for photon energies up to $\sim$6 keV. Owing to the fact that the XRS/EBIT calorimeter array operates at 60 mK, it must be shielded from higher-temperature sections of the spectrometer. This is achieved via four aluminized polyimide blocking filters. In addition, there is an insertable aluminized polyimide filter mounted between the EBIT-I and the XRS/EBIT. This filter was used to reduce flux from low-energy photons. The combined thickness of the filters is 3824 Å of aluminum and 14310 Å of polyimide. The relative X-ray transmission efficiency through these filters for the photon energies studied here is 3%. The XRS/EBIT viewed the trapped ions through one of EBIT-I's six radial ports oriented at 90° to the electron beam. Neutral argon gas is introduced to the trap continuously via a differentially pumped, collimated ballistic gas injector, which is also attached to one of the six radial ports. Once injected, argon atoms intersect the beam and are then ionized and trapped.

Table 1
The Atomic Data Sources for Argon in AtomDB v2.0.2 and AtomDB v3.0.8. CH = Chianti v7 (Dere et al. 2009)

Ion	Wavelengths	Einstein A	Coll. Exc.	DR Satel.	Inner shell
AtomDB v2.0.2					
Ar^{14+}	CH	CH	CH	None	None
Ar^{15+}	CH	CH	CH	None	None
Ar^{16+}	D, W	W	W	VS	None
Ar^{17+}	E, AS	AS	FAC	VS	None
AtomDB v3.0.8					
Ar^{14+}	CH	CH	CH	None	P
Ar^{15+}	N	L	CH	None	P
Ar^{16+}	D, W	W	W	VS	FAC
Ar^{17+}	E, N	FAC	LI	VS	None

Note. D = Drake (1988). VS = Vainshtein & Safronova (1980). L = Liang & Badnell (2011). LI = Li et al. (2015). E = Erickson (1977). N = Kramida et al. (2015). P = Palmeri et al. (2008). FAC = flexible atomic code, similar to this work. AS = autostructure (Badnell 2016).

3. Atomic Modeling

3.1. AtomDB

The AtomDB project couples an atomic database with a model of optically thin, collisionally ionized plasma to produce emission spectra predictions for astrophysical plasma. This model is known as the *apec* model in the XSPEC analysis suite (Arnaud 1996) and was used in Bu14a and Bu14b. These papers used AtomDB v2.0.2 models (Foster et al. 2012), while in this work, we use the more recent AtomDB v3.0.8. The atomic data is largely similar between the two, but some fundamental changes to the structure of the database and code have made this later version more suitable to this work.

The AtomDB atomic database consists of data from a wide range of sources for the emissivities. For argon, the ionization and recombination rates are taken from Bryans et al. (2006, 2009). For each ion for Ar^{14+} to Ar^{17+}, we list the sources of other atomic data in Table 1. Note that for each process within each ion, sometimes several different data sources are used based on the coverage of the published data sets. Therefore, in Table 1, we list only those most relevant to the ions and lines observed in this work. All of the atomic data is available online.[6]

The updates to both the atomic data and the underlying structure of AtomDB between version 2.0.2 and 3.0.8 are minor. The changes are adjusted wavelengths to National Institute of Standards and Technology (NIST) values where

[6] http://www.atomdb.org/

Table 2
Integrated Normalized Flux of Ar Lines in a 1.74 keV Maxwellian Plasma from AtomDB v2.0.2 and AtomDB v3.0.8

Line	Energy (keV)	AtomDB v2.0.2	AtomDB v3.0.8	Ratio
Ar XVII Heα	3.080–3.150	11.404	11.420	1.00
Ar XVIII Lyα DR	3.260–3.315	0.378	0.384	0.98
Ar XVIII Lyα	3.315–3.350	2.433	2.424	1.00
Ar XVII Heβ DR	3.600–3.645	0.100	0.097	1.03
Ar XVII Heβ	3.670–3.700	0.849	0.832	1.02
Ar XVII Heγ	3.850–3.900	0.293	0.287	1.02
Ar XVIII Lyβ	3.925–3.945	0.318	0.298	1.07
Ar XVII Heδ	3.950–3.975	0.126	0.123	1.02
Ar XVII He$\epsilon - \iota$	4.000–4.082	0.168	0.176	0.96

Note. Differences to Table 4 are due to the differences in the charge balance between the fitted model and the theoretical Maxwellian plasma.

possible; this has little effect on this work as typical adjustments were on the 1–2 eV range, significantly smaller than the spectral resolution of the instruments in B14a. The more significant update is to include representation of inner-shell excitation and generally to improve representation of nonequilibrium plasma. This involves using published data for inner-shell ionization and fluorescence yields, as well as new Li-like electron collision data to include the effect of the inner-shell excitation. In addition, the plasma calculations are reworked completely. Instead of calculating the emission based on the ion containing the transition (so for the Heα line, looking at Ar^{16+}), the emissivities are broken up by the parent ion. Thus an ion of, say, Ar^{16+} can give rise to lines from Ar XVI due to dielectronic or radiative recombination, Ar XVII due to excitation, and Ar XVIII due to excitation-autoionization or direct ionization. Since emissivity is calculated by ion, it is possible to model the ionization balance found in the EBIT-I's Maxwellian simulation mode.

DR satellite lines are included in AtomDB from Vainshtein & Safronova (1980). This data set includes a capture from H- and He-like Ar ions, but not Li-like. Due to the enhanced Li-like DR line presence, we have added the $1s2s2l3l'$ satellite lines to our model, using the parameters from Table 6 of Beiersdorfer et al. (1995). In addition, the $1s3l3l'$ satellites from the capture from He-like ions is also not in AtomDB v3.0.8, so the data from Table 5 of that paper has also been included. All of these lines lie between 3.54 and 3.69 keV, and therefore could be an additional source of emissivity missing from the models in B14a. These satellite lines, calculated by HULLAC (Bar-Shalom et al. 2001), have been verified experimentally by Beiersdorfer et al. (1995) in similar plasma temperatures to those expected in clusters, i.e., $kT = 2.3$ keV.

3.1.1. Comparison of AtomDB 3.0.8 to AtomDB 2.0.2

It is not possible to analyze the EBIT-I data with AtomDB v2.0.2 due to the structural differences outlined above. We have, therefore, analyzed the data in this paper with AtomDB v3.0.8, and in this section, we explore the differences between AtomDB v2.0.2 and AtomDB v3.0.8 to show that results obtained in this work are similar to what would have happened in B14a.

The effect of changing between these two data sets is shown in Table 2 for a Maxwellian plasma with $kT = 1.74$ keV(see Section 4 for the details on the temperature estimate). The emissivity of the strongest lines changes by less than 5%, so any changes due to this are negligible compared to the factor of 2 difference between the experiment and the AtomDB values. We shall ignore any contributions from this for the remainder of this work.

3.2. The FAC

The FAC (Gu 2004, 2008) is a comprehensive code that calculates energy levels, transition rates, and cross sections. Additionally, the FAC contains a collisional radiative model that estimates the line strengths for optically thin plasmas based on the atomic physics parameters previously calculated with the FAC. The ion abundances, the choice of processes to include, the electron density, and the electron distribution are user input parameters. The electron energy distribution can be chosen freely from predefined functions (e.g., a Gaussian distribution for electron beams and a Maxwellian distribution for thermal plasmas) or is user-defined through a table model.

Here, we used the FAC to calculate the energy levels for H-like to B-like Ar for configurations of the form: $n\ell$ (H-like); $1s^2$, $1s\,n\ell$, $2\ell\,2\ell'$, and $2\ell\,n\ell'$ (He-like); $1s^2\,2\ell^x$, $1s^2\,2\ell^{x-1}\,n\ell'$, $1s\,2\ell^y$, and $1s\,2\ell^{y-1}\,n\ell'$ (Li- to B-like), allowing for spectator electrons up to n = 5. Transition rates and cross sections were calculated for transitions between any of these configuration groups. We then used the data to calculate the plasma model at temperatures in the range of 1.2–3.0 keV, including radiative decay, collisional (de-)excitation and ionization, radiative recombination, DR, and autoionization. For the relative ion abundances, we used the FAC's default charge balance at the respective temperatures. The Maxwellian electron energy distribution for each temperature was integrated between 50 eV and 20 keV, and an electron density of 1×10^{11} cm^{-3} was assumed. We then convolved the resulting line strengths for each transition with a Gaussian line profile of 5.0 eV FWHM to produce the final spectrum.

To obtain the theoretical DR/Lyα line ratio, we then summed the spectra in the range of 3250–3307 eV for the DR lines and 3307–3340 eV for the Lyα lines, such that the unresolved DR resonance blending with the Lyα lines are included in the line ratio. Neglecting the unresolved blends to Lyα would falsely result in an increase of the ratio of between 23% at 1.2 keV and 6% at a 3.0 keV electron temperature.

4. Results

The electron temperature of the EBIT-I plasma is determined using the line ratio of the Ar XVIII Lyα DR lines to their parent Ar XVIII Lyα line (Gu et al. 2012). This method has been well tested and only relies on the presence of hydrogenic ions. Figure 1 shows the temperature dependence of this ratio given by AtomDB v3.0.8 and the FAC. Before comparing the measured ratio to the theory, polarization effects must be taken into account. As a result of the unidirectional electron beam, electron beam ion traps produce non-isotropic, polarized radiation that depends on both electron impact energy and transition (Beiersdorfer et al. 1996; Gu et al. 1999). This effect is reduced by the fact that electrons in the beam have a spiral trajectory caused by their thermal velocity when they are generated at the electron gun. In general, polarization is

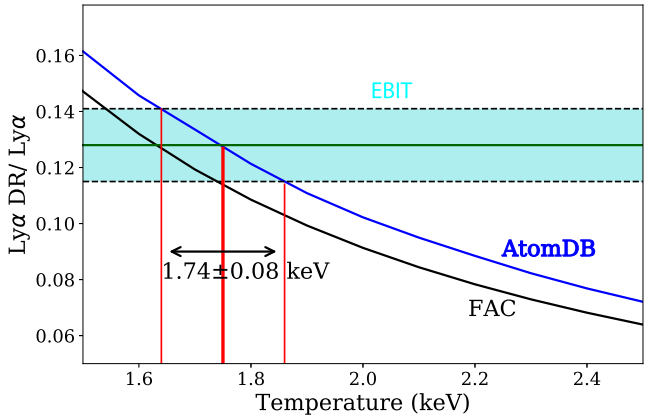

Figure 1. AtomDB v3.0.8 and FAC predicted temperature dependence of the Ar XVIII Lyα DR to the Ar XVIII Lyα lines are shown. The line ratio is compared with the EBIT measurement with its uncertainty limits (shaded cyan region). AtomDB v3.0.8 predictions show that the EBIT measurements are consistent with a Maxwellian temperature of $T_e = 1.74 \pm 0.08$ keV.

reduced as a function of electron impact energy. The polarization of Lyα1 is measured to be $\sim$0.1 by Nakamura et al. (2001). This result is consistent with a more recent theory (Bostock et al. 2009). In the case of the DR emission, a range of polarization values are predicted owing to the fact that several transitions of the type 1s 2ℓ make up this feature. The DR features consist of several transitions with a range of polarization values, most of which are positive. Using the calculations of Chen & Scofield (1995) as a guide, we assign an average value of $P = 0.5$ to all of the H-like Ar DR satellites. Because of the depolarizing effect of the spiraling beam and the fact that the electron beam energy is swept across a large range for these measurements, we make no correction for polarization for this ratio and assign an uncertainty resulting from polarization in the ratio of $\pm$10%. This is determined by nearly the full range of polarization correction factors, including the possibility of the DR polarization being largely negative. This uncertainty, combined with the statistical uncertainty of $\sim$7%, gives a ratio of the Ar XVIII Lyα DR line to the parent line of 0.135 ± 0.016. This ratio corresponds to a plasma temperature of 1.74 ± 0.08 keV based on the AtomDB model and 1.64 ± 0.08 keV based on the FAC model (see Figure 1).

Using the Maxwellian temperature of $kT_e = 1.74$ keV, we calculate the spectra created by Ar^{14+}–Ar^{18+} using AtomDB v3.0.8. The lines are broadened with a FWHM of 5 eV to match the observed EBIT calorimeter response. In a true Maxwellian plasma, such as is expected in the central region of galaxy clusters, the charge state distribution for a $kT_e = 1.74$ keV plasma would be multiplied by each ion's emissivity, i.e.,

$$\mathrm{Counts_{tot}}(E) = C \sum^{z1} \varepsilon_{z1}(E) N_{z1}, \quad (1)$$

where C is a constant coefficient incorporating the volume, number density of electrons and argon ions, and detector efficiency; $\varepsilon(E)$ is the emissivity in each energy bin, E; and N_{z1} is the fraction of argon ions in ion state $z1$, where $z1$ is the ion charge $+1$.

As we do not have an ionization equilibrium charge state distribution in a plasma with constituents that have Maxwellian velocity distributions in the measurement, we determine the ion

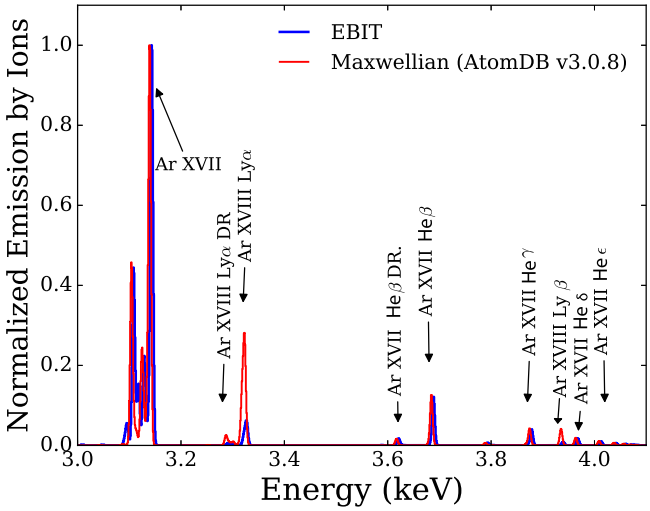

Figure 2. Comparison of the Ar emission spectrum obtained from the EBIT and the modeled Maxwellian plasma obtained from AtomDB v3.0.8 in the full 3–4 keV energy band. The normalized y-axis is normalized to the Ar XVII resonance line. The EBIT spectrum is shifted by +5 eV to show the difference between the AtomDB v3.0.8 and EBIT spectra. The emission lines from different Ar species are marked on the spectrum. Large discrepancies in the Ar XVIII lines are due to the non-Maxwellian equilibrium ionization balance in the EBIT, which is assumed in the AtomDB spectrum.

Table 3
The Ion Fraction (C_{z1}) Obtained from a Theoretical Maxwellian and for Fits to the EBIT Spectrum

Ion	Maxwellian	EBIT (AtomDB)	EBIT (FAC)
Ar^{13+} (B-like)	0.000	0.000	0.017
Ar^{14+} (Be-like)	0.001	0.087	0.087
Ar^{15+} (Li-like)	0.024	0.144	0.289
Ar^{16+} (He-like)	0.577	0.681	0.513
Ar^{17+} (H-like)	0.330	0.086	0.094
Ar^{18+} (fully stripped)	0.068	0.001	0.001

charge states by treating each ion as if it had an independent scaling factor, i.e.,

$$\mathrm{Counts_{tot}}(E) = \sum^{z1} C_{z1} \varepsilon_{z1}(E) N_{z1}, \quad (2)$$

and then fit the data in the 3–4 keV band to these spectra to obtain C_{z1}. The ratio of these determines the charge state distribution. We obtain best-fit ion fractions, as shown in Table 3, showing a significant increase in the Li-like Ar fraction in the EBIT at the expense of the H-like stage compared with a Maxwellian plasma.

In Figure 2, we show the spectrum of a 1.74 keV plasma from AtomDB v3.0.8 and the observed EBIT spectrum, labeling the strong lines of Ar. We stressed that the EBIT spectrum is artificially shifted by +5 eV to show the difference between AtomDB v3.0.8 and the measured EBIT spectra. As can be seen, there is a significant difference in the Lyman series line intensities as there are many fewer Ar^{17+} ions in EBIT than predicted for a Maxwellian charge distribution. Figure 3 compares the spectra for four different energy ranges between the EBIT and the spectrum with the fitted EBIT ion ratios (e.g., 3.08–3.16 keV, 3.2–3.4 keV, 3.6–3.7 keV, and 3.85–4.1 keV). It shows that the model is generally a good fit to the observed data: in particular, the Lyα lines as well as the Heα, Heβ, and

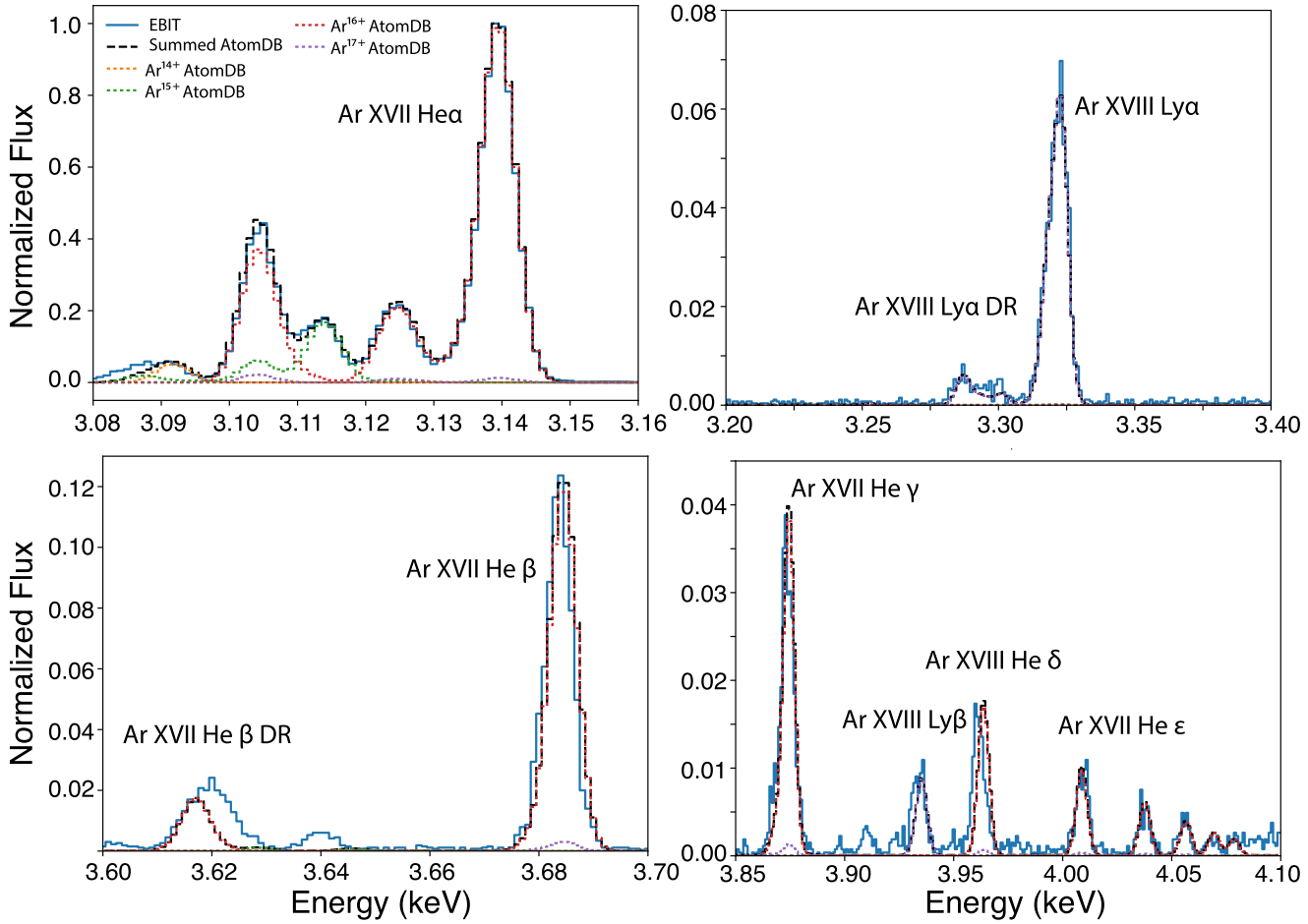

Figure 3. Zoomed-in energy bands of the AtomDB v3.0.8 and EBIT spectra. The figure compares the EBIT results (solid blue line) with the emission from each ion of argon calculated using AtomDB v3.0.8 with the ion fractions for the EBIT plasma from Table 3.

Table 4
Integrated Normalized Flux in the EBIT Experiment and Modeled Plasma

Line	Energy (keV)	Experiment	AtomDB v3.0.8	Ratio	FAC
Ar XVII Heα	3.080–3.150	1.00e+00	1.00e+00	1.000	1.00e+00
Ar XVIII Lyα DR	3.260–3.315	1.06e-02	6.92e-03	1.533	2.13e-02
Ar XVIII Lyα	3.315–3.350	4.35e-02	4.19e-02	1.037	4.33e-02
Ar XVI Kβ	3.539–3.600	5.21e-03	9.83e-04[a]	5.297	5.62e-03
Ar XVII Heβ DR	3.600–3.645	2.31e-02	9.77e-03	2.359	2.43e-02
Ar XVII Heβ DR$_1$	3.600–3.630	1.94e-02	9.43e-03	2.057	2.21e-02
Ar XVII Heβ DR$_2$	3.630–3.645	3.65e-03	3.39e-04	10.746	2.10e-03
Ar XVII Heβ	3.670–3.700	5.98e-02	6.29e-02	0.952	5.49e-02
Ar XVII Heγ	3.850–3.900	2.30e-02	2.19e-02	1.051	2.48e-02
Ar XVIII Lyβ	3.925–3.945	6.19e-03	4.60e-03	1.346	3.72e-03
Ar XVII Heδ	3.950–3.975	9.70e-03	8.88e-03	1.092	7.78e-03
Ar XVII He $\epsilon \rightarrow \iota$	4.000–4.082	1.33e-02	1.27e-02	1.051	⋯

Note.
[a] With added DR lines (Section 4.1), 4.27e-03.

Heγ. There is a noticeable discrepancy at 3.62 keV, which is the Ar DR line we are studying.

For the given charge balance in the EBIT-I Maxwellian plasma, ignoring polarization effects, the ratio of He-β DR to He-$\beta_{1,2}$ is 0.36 ± 0.02 where the error is given by the quadrature sum of background subtraction and statistics. If we assume maximum polarization for He-β_1 of $P = 0.63$ (Smith et al. 1996) and for the DR satellites of 0.4, the ratio becomes 0.4, i.e., it changes by 10% (Smith et al. 2000). However, owing to the fact that the beam dynamics are not well known and that the polarization was not measured in situ, the correction for polarization is not well known. Thus we assume the maximum polarization effect in deriving the uncertainty in these measurements.

In Table 4, we list the total normalized flux in each of the 12 energy bands from both the theoretical and observed EBIT spectra, each corresponding to a different line. The fluxes are normalized to the Ar XVII He-α feature flux for each spectrum.

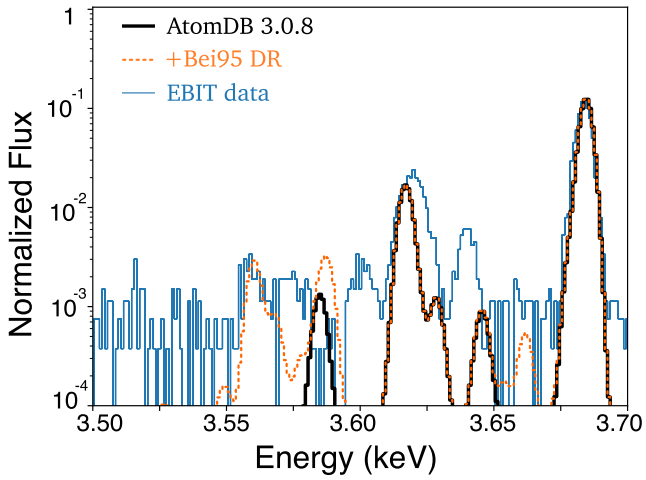

Figure 4. Spectrum of a 1.74 keV plasma, assuming the ion abundances of Table 3 and AtomDB v3.0.8 (solid black line). The orange dotted line shows the same with the DR satellite lines from Beiersdorfer et al. (1995) added. EBIT experimental data is shown in blue.

The ratios for the non-DR lines are within 10% of their predicted values, with the exception of the weak Lyβ feature at 3.935 keV, which is 35% stronger in the experimental data. The DR lines for both Ar XVII and Ar XVIII are significantly stronger in the EBIT experiment than predicted by our fit model, by factors of 2.4 and 1.5, respectively. This is traced to missing satellite transitions in each band.

4.1. Effect of Additional DR Satellite Lines

In this section, we discuss the effects of adding a range of additional DR satellite lines on our results. In the first case, we added the HULLAC data discussed in Section 3.1. Including and removing these had no noticeable change on the ion fractions of Table 3, with the change in each relative ion fraction being less than 1%. Where this does make a difference is the Ar XVIDR satellites in the 3.55–3.59 keV band. These significantly improve the fit between the EBIT and theoretical data. Figure 4 shows Ar XVIXVI DR satellite lines in the 3.5–3.7 keV band, the only region with any significant change. The fluxes of these added lines are still significantly weaker than required to account for the 3.5 keV line flux observed in clusters: they amount to 25% of the flux in the 3.62 keV line, which is itself too small. Therefore, this neither explains the 3.55 keV feature in B14a nor explains the extra flux in the Ar XVII Heβ DR lines.

Guided by the lower temperature obtained from the FAC data fit than from the AtomDB fit (1.64 keV versus 1.74 keV), we have also investigated a range of electron temperatures in the 1.5 to 1.8 keV range. These yield no significant change (<2% difference) in the ion fractions and no significant change in the resulting flux ratios in the 3.62 keV region. Additionally, adjusting the wavelength of the DR satellite lines to match the 3.62 keV line more closely does not lead to any significant change in the modeled ion fractions or line fluxes in this region, as the line's modeled emissivity is constrained by the 3.68 keV line.

4.2. Comparison with FAC Data

In an effort to identify the 3.64 keV feature, which was not in the AtomDB data, we used the FAC data already calculated to predict this feature, as shown in Figure 5. The results of this suggest the 3.64 keV feature is largely driven by $1s2p3[pd] \rightarrow 1s^2 2p$ transitions in the Li-like ion. These satellites are not included in the work of Vainshtein & Safronova (1980), which explains their absence from the AtomDB v3.0.8 spectrum.

4.3. Comparison with Bulbul et al. (2014a)

One of the suggested interpretations of the 3.5 keV line is an unexpectedly strong Ar XVII Heβ DR dielectronic recombination satellite line created by recombining He-like Ar XVII at 3.62 keV. Indeed, if the Ar XVII Heβ DR line is 30 times stronger than the predicted strength in AtomDB v2.0.2, this would explain the excess observed in the stacked clusters (see B14a). The line ratios and line fluxes presented in this work correspond to a Maxwellian plasma with a 1.74 keV temperature that is similar to the intracluster medium (ICM) temperatures of cool-core clusters. In this section, we fit the *XMM-Newton* spectra of the stacked clusters of galaxies in B14a with the new EBIT measurements to measure the effect of atomic database changes to the detection of the 3.5 keV line.

In the fits of the B14a stacked sample (and in all other samples), the maximum flux for the Ar XVII Heβ DR line at 3.62 keV was initially set to 1% of the Ar XVII Heα line at 3.12 keV in the spectral fits. The 3.62 keV flux was allowed to go a factor of three above these estimates as a safety margin to account for the uncertainties in the emissivities of the weak DR lines. The upper limit corresponds to the highest flux that Ar XVII Heβ DR can have for the lowest ICM plasma temperature (2 keV) observed in B14a. For instance, the observed flux measured in the Ar XVII Heα line is 2.1×10^{-5} counts cm^{-2} s^{-1}. The allowed flux upper limit for the Ar XVII Heβ DR line is 6.3×10^{-7} counts cm^{-2} s^{-1}, which is in the limits of the observed ratio by the EBIT. Indeed, by fitting the 3–6 keV band of the *XMM-Newton* Metal Oxide Semi-conductor (MOS) CCD array spectrum of the stacked cluster sample with the new ratios indicated by the EBIT-I experiment, the 3.5 keV line is still detected at a 5σ confidence level with a flux of $3.98 \pm 0.7 \times 10^{-6}$ photons cm^{-2} s^{-1}. Therefore, we rule out that the excess emission observed in the stacked clusters and the Perseus cluster is due to the satellite Ar XVII Heβ DR lines in the 3.5–3.7 keV energy band.

5. Conclusions

We present lab measurements of the Ar^{14+}–Ar^{18+} spectra using the EBIT-I facility located at LLNL. We obtain a detailed spectrum, including faint dielectronic satellites lines, and compare the emissivities with the atomic calculations in the atomic database AtomDB v3.0.8. Our major results are as follows:

1. We find that the EBIT-I data from a pseudo-Maxwellian plasma of highly charged argon ions are consistent with an ionization temperature of $T_e = 1.7$ keV for a plasma with a Maxwellian electron distribution. This temperature is comparable to the plasma temperatures observed in cool-core galaxy clusters; therefore, EBIT-I Ar flux measurements can directly be compared to the X-ray data in B14a.
2. The EBIT-I data are consistent with the predictions of the He-like Ar lines and Heα, Heβ, and Heγ emissivities of the model within 10%.

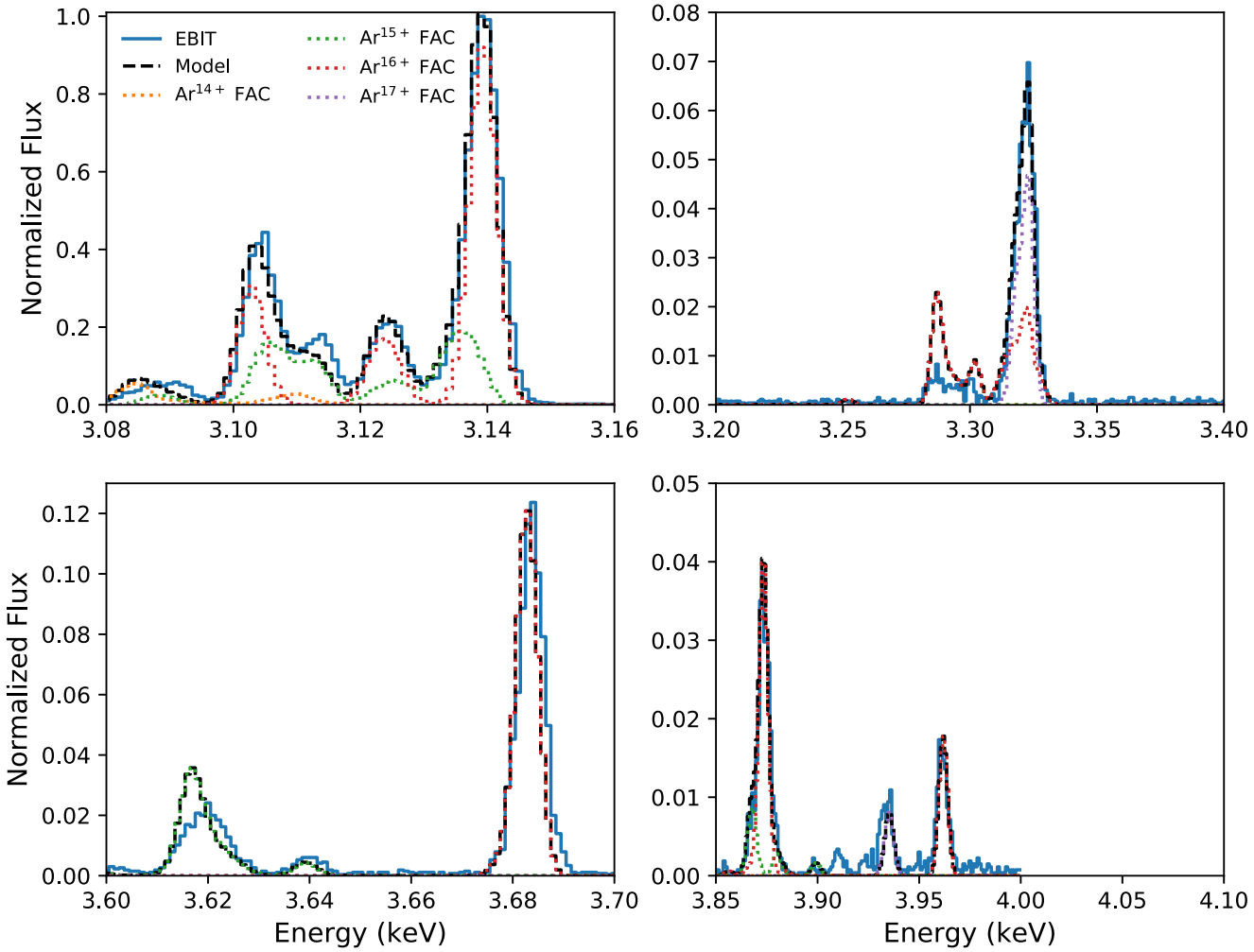

Figure 5. Same as Figure 3, but using the FAC to generate the spectrum. The 3.64 keV line is modeled well, though several other features are less well recreated. The spectral model truncates at 4 keV.

3. We have identified new satellite lines in the 3.5–3.7 keV band. These additional lines, however, are too weak to resolve the flux discrepancies near 3.5 keV line as their fluxes are ∼0.5% of that of Ar XVII Heα line. These have been attributed to the $1s2p3[pd] \rightarrow 1s^2 2p$ satellite lines.
4. The measured flux in the Ar XVII He-β DR line is 2.4 times higher than that predicted in AtomDB v3.0.8. However, a factor of 3 safety margin was allowed in B14a to account for uncertainties in the satellite line fluxes. Fitting the *XMM-Newton* spectrum of the stacked clusters sample with the ratios indicated by the new EBIT measurements produces a 3.5 keV line flux of $3.98 \pm 0.7 \times 10^{-6}$ photons $\mathrm{cm}^{-2}\,\mathrm{s}^{-1}$. The unidentified line is still detected at the 5 σ confidence level. These new EBIT measurements rule out the Ar XVII Heβ DR origin of the unidentified emission line detected in clusters of galaxies at 3.5 keV.

The EBIT measurements of charged Ar^{14+}–Ar^{18+} ions presented in this work provide independent tests on theoretical calculations and are essential when interpreting the high-resolution spectra, which will be available through *X-ray Imaging and Spectroscopy Mission* (*XRISM*) and *Athena* X-ray Integral Field Unit (X-IFU) observations (Nandra et al. 2013; Barret et al. 2018).

Authors thank the anonymous referee for helpful comments on the draft. Part of this work was performed under the auspices of the U.S. Department of Energy by Lawrence Livermore National Laboratory under Contract DE-AC52-07NA27344 and supported by NASA contract NNM15AA35I and *Chandra* award AR5-16012Z.

ORCID iDs

Adam Foster https://orcid.org/0000-0003-3462-8886
Peter Beiersdorfer https://orcid.org/0000-0003-0127-599X
Natalie Hell https://orcid.org/0000-0003-3057-1536
Ralph Kraft https://orcid.org/0000-0002-0765-0511
Randall K. Smith https://orcid.org/0000-0003-4284-4167

References

Abazajian, K. N. 2017, PhR, 711, 1
Arnaud, K. A. 1996, in ASP Conf. Ser. 101, Astronomical Data Analysis Software and Systems, ed. G. H. Jacoby & J. Barnes (San Francisco, CA: ASP), 17
Badnell, N. R. 2016, AUTOSTRUCTURE: General Program for Calculation of Atomic and Ionic Properties, Astrophysics Source Code Library, ascl:1612.014
Barret, D., Trong, T. L., den Herder, J.-W., et al. 2018, arXiv:1807.06092
Bar-Shalom, A., Klapisch, M., & Oreg, J. 2001, JQSRT, 71, 169
Beiersdorfer, P. 2008, CaJPh, 86, 1

Beiersdorfer, P., Behar, E., Boyce, K. R., et al. 2003, NIMPB, 205, 173
Beiersdorfer, P., Osterheld, A. L., Phillips, T. W., et al. 1995, PhRvE, 52, 1980
Beiersdorfer, P., Vogel, D. A., Reed, K. J., et al. 1996, PhRvA, 53, 3974
Bostock, C. J., Fursa, D. V., & Bray, I. 2009, PhRvA, 80, 052708
Boyarsky, A., Franse, J., Iakubovskyi, D., & Ruchayskiy, O. 2015, PhRvL, 115, 161301
Boyarsky, A., Ruchayskiy, O., Iakubovskyi, D., & Franse, J. 2014, PhRvL, 113, 251301
Bryans, P., Badnell, N. R., Gorczyca, T. W., et al. 2006, ApJS, 167, 343
Bryans, P., Landi, E., & Savin, D. W. 2009, ApJ, 691, 1540
Bulbul, E., Markevitch, M., Foster, A., et al. 2014a, ApJ, 789, 13
Bulbul, E., Markevitch, M., Foster, A., et al. 2016, ApJ, 831, 55
Bulbul, E., Markevitch, M., Foster, A. R., et al. 2014b, arXiv:1409.4143
Cappelluti, N., Bulbul, E., Foster, A., et al. 2017, arXiv:1701.07932
Chen, M. H., & Scofield, J. H. 1995, PhRvA, 52, 2057
Conlon, J. P., Powell, A. J., & Marsh, M. C. D. 2016, PhRvD, 93, 123526
Dere, K. P., Landi, E., Young, P. R., et al. 2009, A&A, 498, 915
Drake, G. W. 1988, CaJPh, 66, 586
Erickson, G. W. 1977, JPCRD, 6, 831
Foster, A. R., Ji, L., Smith, R. K., & Brickhouse, N. S. 2012, ApJ, 756, 128
Franse, J., Bulbul, E., Foster, A., et al. 2016, ApJ, 829, 124
Gu, L., Kaastra, J., Raassen, A. J. J., et al. 2015, A&A, 584, L11
Gu, M. F. 2004, in AIP Conf. Ser. 730, Atomic Processes in Plasmas, ed. J. S. Cohen, D. P. Kilcrease, & S. Mazavet (Melville, NY: AIP), 127
Gu, M. F. 2008, CaJPh, 86, 675
Gu, M. F., Beiersdorfer, P., Brown, G. V., et al. 2012, CaJPh, 90, 351
Gu, M. F., Savin, D. W., & Beiersdorfer, P. 1999, JPhB, 32, 5371
Kelley, R. L., Akamatsu, H., Azzarello, P., et al. 2016, Proc. SPIE, 9905, 99050V
Kramida, A., Ralchenko, Yu., Reader, J. & NIST ASD Team 2015, NIST Atomic Spectra Database v.5.3 (Gaithersburg, MD: NIST), https://physics.nist.gov/asd
Levine, M. A., Marrs, R. E., Henderson, J. R., Knapp, D. A., & Schneider, M. B. 1988, PhST, 22, 157
Li, S., Yan, J., Li, C. Y., et al. 2015, A&A, 583, A82
Liang, G. Y., & Badnell, N. R. 2011, A&A, 528, A69
Marrs, R. E. 2008, CaJPh, 86, 11
Marrs, R. E., Levine, M. A., Knapp, D. A., & Henderson, J. R. 1988, PhRvL, 60, 1715
May, M. J., Beiersdorfer, P., Jordan, N., et al. 2005, NIMPB, 235, 231
May, M. J., Beiersdorfer, P., Schneider, M., et al. 2004, in AIP Conf. Ser. 730, Atomic Processes in Plasmas, ed. J. S. Cohen, D. P. Kilcrease, & S. Mazavet (Melville, NY: AIP), 61
Nakamura, N., Kato, Miura, D. N., Nakahara, T., & Ohtani, S. 2001, PhRvA, 63, 024501
Nandra, K., Barret, D., Barcons, X., et al. 2013, arXiv:1306.2307
Neronov, A., Malyshev, D., & Eckert, D. 2016, PhRvD, 94, 123504
Palmeri, P., Quinet, P., Mendoza, C., et al. 2008, ApJS, 177, 408
Porter, F. S., Audley, M. D., Beiersdorfer, P., et al. 2000, Proc. SPIE, 4140, 407
Porter, F. S., Brown, G. V., Boyce, K. R., et al. 2004, RScI, 75, 3772
Savin, D. W., Badnell, N. R., Beiersdorfer, P., et al. 2008, CaJPh, 86, 209
Savin, D. W., Beiersdorfer, P., Kahn, S. M., et al. 2000, RScI, 71, 3362
Smith, A. J., Beiersdorfer, P., Decaux, V., et al. 1996, PhRvA, 54, 462
Smith, A. J., Beiersdorfer, P., Widmann, K., Chen, M. H., & Scofield, J. H. 2000, PhRvA, 62, 052717
Takahashi, T., Kokubun, M., Mitsuda, K., et al. 2016, Proc. SPIE, 9905, 99050U
Urban, O., Werner, N., Allen, S. W., et al. 2015, MNRAS, 451, 2447
Vainshtein, L. A., & Safronova, U. I. 1980, ADNDT, 25, 311